Invariant Tori for Two-Dimensional Non-integrable Hamiltonians*

M. A. M. DE AGUIAR† AND M. BARANGER

Center for Theoretical Physics,
Laboratory for Nuclear Science, and Department of Physics,
Massachusetts Institute of Technology, Cambridge, Massachusetts 02139

Received May 24, 1988

The invariant tori of a two-dimensional non-integrable Hamiltonian form families which can be parametrized by the energy and the rotation number. Within each family, the variation with energy is continuous, and the variation with rotation number is governed by the KAM theorem and is everywhere discontinuous. In order to calculate the tori numerically, we approximate them by highly winding periodic orbits, and we give a criterion for the validity of this approximation. For one particular Hamiltonian, we study the family of tori which connects two distinct families of periodic trajectories. As a by-product of this calculation, we draw the curve bounding the "mostly regular" region, on a plot whose coordinates are the two partial periods of the tori.

I. INTRODUCTION

In this paper we present a method to calculate invariant tori in two-dimensional non-integrable Hamiltonian systems. In these systems, two-parameter families of irrational tori are found in the neighborhood of every one-parameter branch of stable periodic orbits. These families can actually be labeled by the (stable) periodic orbit which they surround. Buried among these irrational tori, in the places where the rational tori should have been, we find instead an even number of periodic trajectories, half stable and half unstable [1].

These are the very trajectories that our method uses as approximations to the actual (irrational) tori. The danger of this procedure is that periodic orbits can exist at all energies, while a torus will eventually be destroyed as we increase energy along its family. This means that our approximation will break down at some point. As we shall see later, this is not a drawback at all. On the contrary, it gives us additional information concerning the boundary between the region of phase space containing this particular family and the rest of phase space. The advantages of working with periodic orbits instead of actual tori are obvious: they are one-dimen-

* This work is supported in part by funds provided by the U.S. Department of Energy (DOE) under Contract DE-AC02-76ER03069.

† Supported by Conselho Nacional de Desenvolvimento Científico e Tecnológico.

0003-4916/88 $7.50

595/186/2-10

sional objects and can be completely known in a finite interval of time. Besides, at least for two-dimensional Hamiltonians, the stability of the orbit can be extracted just by calculating the trace of its monodromy matrix [2].

The use of periodic trajectories to study the behavior of nearby invariant surfaces is not new. Some of the ideas presented here have already been discussed for two-dimensional area-preserving maps [3]. The new feature of this work is that, here, the periodic orbits are themselves used to approximate tori and not only to study their qualitative behavior.

Two other basically different approaches to calculate tori are known to the authors, neither of which make use of periodic orbits. In the first [4] the Hamiltonian is supposed to be quasi-integrable, so that particles propagated from almost all possible initial conditions will be on tori. Poincaré sections of these orbits are used to find the basic circuits with which to calculate the actions. The second approach [5] is a rapidly convergent procedure to solve the Hamilton–Jacobi equation in terms of its Fourier coefficients. Although the latter method seems to give excellent results, both procedures have the disadvantage that they are unable to calculate families of tori other than those existing in the integrable (usually zero energy) limit.

The numerical calculations in this paper use the Hamiltonian

$$H(x, y, p_x, p_y) = \frac{p_x^2}{2} + \frac{p_y^2}{2} + \frac{x^2}{2} + \frac{3y^2}{2} - x^2 y + \frac{x^4}{12}, \tag{1.1}$$

for which our code name is MARTA. An extensive numerical study of its periodic orbits can be found in Ref. [6]. Our results will be presented here in the form of plots of J_1 versus J_2, the two independent actions of a two-dimensional torus, plots of τ_1 versus τ_2, the two partial periods around the corresponding topologically independent circuits, and y versus x projections of the objects themselves.

In Section II we shall discuss the intimate relation between tori and periodic orbits for non-integrable systems. We show, in particular, that the irrational tori which survive the KAM destruction can be approximated as precisely as we wish by periodic orbits of long period. In Section III we derive a quantitative criterion to measure how good this approximation is in generic Hamiltonian systems. When the approximation is good, the periodic orbit will be called a "quasi-torus" and, when it is not, it will be called a "main periodic orbit." The construction of the two basic loops and the calculation of the actions are discussed in Section IV, and the numerical results for the MARTA Hamiltonian are presented in Section V. Finally, in Section VI we summarize our conclusions.

Before closing this introduction, we recall that the basic motivation for this work is the quantization of non-integrable Hamiltonians. A series of recent works (Ref. [7]) shows that the exact eigenstates, the quantum stationary objects, can be related to either periodic orbits, tori, or chaotic regions, which, in a sense, are the stationary classical structures. Periodic orbits were extensively discussed in Refs. [6, 8, 9]. In this work, we provide tools for a systematic study of tori.

II. Invariant Tori and Periodic Trajectories

Consider a two-dimensional Hamiltonian system of the form

$$H(p_1, p_2, q_1, q_2) = H_0(p_1, p_2, q_1, q_2) + \varepsilon H_1(p_1, p_2, q_1, q_2),$$

where H_0 is integrable, but H is non-integrable for $\varepsilon \neq 0$. The phase space structure of the solutions of H_0 is well known: it consists of nested two-dimensional invariant surfaces with the topology of tori. The conventional way of labeling the tori is by the action variables J_1, J_2. Other pairs of labels are possible, such as the energy E and the rotation number

$$\rho = \omega_2/\omega_1 = (\partial H_0/\partial J_2)/(\partial H_0/\partial J_1). \tag{2.1}$$

If we think of a torus as a donut, then the rotation number measures how many times the particle winds around one of the circles, while performing exactly one rotation around the other circle (see Section IV for more details). If ρ is rational, we say that the torus is rational, and then it is covered by a single infinite family of periodic trajectories, all with the same actions, energy, period, and rotation number. If ρ is irrational, the torus is covered by a single non-closing trajectory commonly known as quasi-periodic. For integrable Hamiltonians, the tori form a continuous two-dimensional family: given a torus labelled by the pair (E, ρ), we can always find two others with parameters $(E+\delta E, \rho)$ and $(E, \rho+\delta\rho)$. If we fix E and vary ρ, we find that the resulting one-dimensional family of tori is bounded by two simple periodic trajectories. This is obvious if we think in terms of action variables. One boundary corresponds to $J_1 = 0$ and the other to $J_2 = 0$.

Now, consider the case $\varepsilon \neq 0$, but very small. Then the KAM [10] and Poincaré–Birkhoff [1] theorems tell us that every rational torus is destroyed and replaced by a finite even number of periodic trajectories, half of them stable and half unstable. Surrounding the stable orbits we find the so-called second order tori, and in the neighborhood of the unstable orbitrs we find a thin chaotic layer. The situation is best visualized in a Poincaré section, as shown in Fig. 2.1.

Therefore, for any $\varepsilon \neq 0$, the two-dimensional family of tori, although still continuous in the energy variable E, becomes discontinuous in the rotation number ρ. In the limit $\varepsilon \to 0$, the chain of islands shown in Fig. 2.1b becomes very thin, and so does the chaotic layer surrounding each of the hyperbolic points which separate the islands. The precise way in which this happens is stated in the KAM theorem. In this limit, the ρ-dependence of the family of tori recovers its continuity.

When $\varepsilon = 0$, it is clear that any irrational torus can be approximated, as well as one wishes, by a rational torus, and therefore by a periodic trajectory. For instance, ρ can be approximated by its continued fraction expansion [11], limited to a finite number of terms. When ε is small but finite, the periodic orbits can still be used to approximate the actual tori, *as long as the* KAM *layer of islands and chaos is thin enough.* We shall need a criterion to determine whether this approximation is good or not, and such a criterion will be given in Section III. For fixed ε, we know [12]

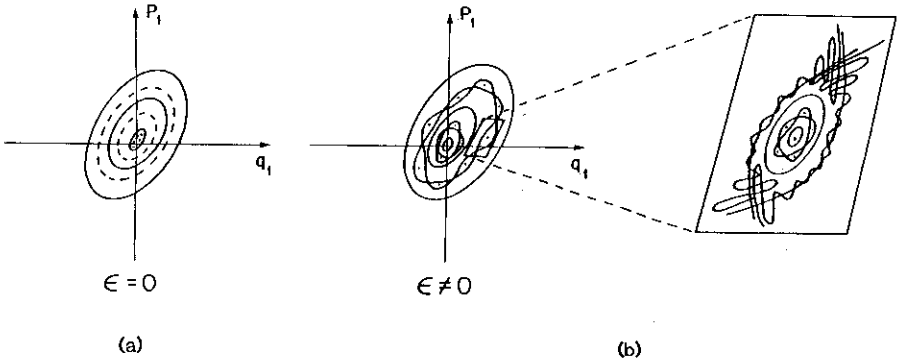

FIG. 2.1. Poincaré section in the neighborhood of a stable periodic orbit. In part (a) $\varepsilon = 0$ and the system is integrable (the dotted lines represent rational tori). In part (b), with $\varepsilon \neq 0$, islands and chaotic layers show up replacing the rational tori.

that the families of periodic trajectories are continuous and can end only at the stationary points of H. The families of tori, on the other hand, are gradually destroyed as the term εH_1 gains in importance (e.g., as the energy increases), and our criterion should be able to tell us whether a periodic orbit is still remaining close to primary tori, to which it is a good approximation, or whether it is not.

Therefore, instead of calculating actual tori, we shall calculate "quasi-tori" objects, which are the objects left by the KAM destruction operating on a rational torus, in the case where this KAM destruction is a mild one; in other words, we shall calculate periodic trajectories which are good approximations to the tori! Usually, these will be high-period orbits which wind many times before closing. There are many advantages to working with periodic orbits instead of non-periodic ones, as we shall see later. The most interesting advantage is that we can learn about what is goind on in the neighborhood of the orbit just by looking at the trace of the monodromy matrix.

How many families of tori are there in a non-integrable Hamiltonians system? We know that we have tori in the neighborhood of every stable periodic orbit and that non-integrable systems can have many families of such orbits [6, 8]. So, if we associate a two-parameter family of tori with every one-parameter family of stable periodic orbits, we may want to answer the following question: do families of tori connect together families of periodic orbits which are not connected on their $E-\tau$ (energy versus period) plot? To answer this, we must study the topology of the families of tori in a way similar to what we did for periodic trajectories [6, 8].

It must be emphasized that the "connection" through the space of tori has to be quite different from the "connection" within periodic trajectories. In the latter case, a connection between two trajectories means that there is a continuous path between the two on the $E-\tau$ plot, usually going through some branch points. In the former case, the connection cannot be continuous since, when we vary ρ, the KAM theorem says that we have to skip the rational values, as well as an irrational

neighborhood of each rational value. In practice, this connection is accomplished by making small but finite jumps from one "quasi-torus" to another. Figure 5.2 is an example of such a connection, through quasi-tori, between the horizontal and vertical families of MARTA (see Section V, Fig. 5.1, and Ref. [6]). Note that the periodic orbits themselves do not connect at low energy.

There are many ways in which this connection can be displayed. Figure 5.2 shows the xy projections of the tori (actually highly winding periodic orbits) at fixed energy. Another obvious choice of coordinates is (J_1, J_2), the actions, given by

$$J_i = \oint_{\Gamma_i} p\, dq, \qquad i = 1, 2,$$

where Γ_1 and Γ_2 are topologically equivalent to a pair of basic loops on the torus (see Section IV for more details). On such a plot, the connection between two periodic families through tori at contant energy should begin on one of the periodic orbits at $(J_1, 0)$, end on the other at $(0, J_2)$, and in between it should proceed by small jumps in the J_1, J_2 plane. If the fraction of KAM-destroyed tori is small, the connecting line should approximate a continuous curve. Such a graph is shown in Fig. 2.2. At each point, the slope of the normal to the energy contour is

$$\tan \varphi = (\partial H/\partial J_2)/(\partial H/\partial J_1) = \omega_2/\omega_1 = \rho.$$

The points where ρ is rational represent KAM-destroyed tori, and these are the points that we can calculate. Most of the points with irrational ρ represent real existing tori, but not all of them, because all tori are destroyed in a small neighborhood of a rational torus [10]. We can think of the points with rational $\tan \varphi$ as holes in the energy contour for tori. Each hole has a width equal to the size of the destroyed neighborhood. When E increases, the size of all the holes

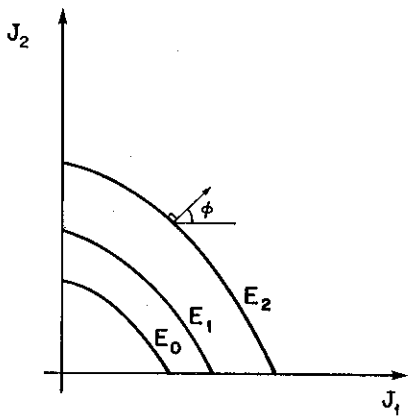

FIG. 2.2. J_1 versus J_2 plot for an integrable Hamiltonian.

increases, and some holes merge with their neighbors, thus putting an end to some irrational regions. In the holes, secondary tori and chaotic motion set in. As energy increases, our initially "well behaved" surface representing a two-dimensional family of tori becomes torn more and more severely: the motion is less and less "regular," more and more "chaotic." According to the KAM theorem, the simpler the rotation number, the bigger the size of the destroyed neighborhood. "Simple" here means a short continued fraction expansion. Because the simple rational numbers are sprinkled in an irregular way among the less simple ones, the pattern of holes is very complicated, and so is the boundary between the regular and chaotic region. Indeed, this boundary is a fractal.

Instead of this boundary, we shall calculate in Section V the simpler boundary between what we shall call there the "mostly regular" region and the rest of phase space. For reasons that will become clear later, the (J_1, J_2) plot is not the best way to see this boundary, and we shall have to introduce new variables for this purpose.

III. Quasi-Tori and Main Periodic Orbits

The purpose of this section is to discuss the neighboring orbits of a given stable periodic trajectory. In particular, we need a criterion to decide when a neighboring peridic orbit is a quasi-torus (i.e., it is a good apprimation for nearby tori) and when it is not. Although the neighborhoods of periodic trajectories in Hamiltonian systems have been discussed extensively in Refs. [6, 8, 9], we shall list here some results which are crucial for the following discussion.

It is well known that periodic trajectories occur in one-parameter families. The parameter can be the energy E or the period τ. For each trajectory, we can calculate the monodromy (or Lyapunov) matrix, which describes what is going on for neighboring trajectories. Using $w(t)$ to denote the four phase space variables,

$$w(t) \equiv \{x(t), y(t), p_x(t), p_y(t)\}, \tag{3.1}$$

we can write the equations of motion in the form

$$\dot{w} = J\nabla H(w), \tag{3.2}$$

where H is the Hamiltonian and J is the symplectic matrix,

$$J = \begin{pmatrix} 0 & 0 & 1 & 0 \\ 0 & 0 & 0 & 1 \\ -1 & 0 & 0 & 0 \\ 0 & -1 & 0 & 0 \end{pmatrix}. \tag{3.3}$$

If $w_0(t)$ is a periodic solution of (3.2) with period τ_0, its monodromy matrix is

obtained as follows. We linearize (3.2) in the vicinity of w_0 by writing $w = w_0 + \xi$. To first order in ξ, we get

$$\dot{\xi} = JH^{**}(t)\,\xi, \tag{3.4}$$

where

$$H_{ij}^{**}(t) = \left.\frac{\partial^2 H}{\partial w_i\,\partial w_j}\right|_{w_0(t)}.$$

If we write the solution of (3.4) in the form

$$\xi(t) = M(t)\,\xi(0), \tag{3.5}$$

then $\mathcal{M} \equiv M(\tau_0)$ is the 4×4 monodromy matrix for w_0.

The monodromy matrix always has two of its eigenvalues, say λ_1 and λ_2, equal to 1. The two other eigenvalues have product unity, $\lambda_3\lambda_4 = 1$. Because $\mathcal{M}$ is real, only two cases are possible:

$$\text{(a)}\quad \lambda_3 = e^{2\pi i\alpha}, \qquad \lambda_4 = e^{-2\pi i\alpha}, \qquad \alpha \text{ real} \tag{3.6a}$$

$$\text{(b)}\quad \lambda_3 = \lambda, \qquad \lambda_4 = 1/\lambda, \qquad \lambda \text{ real.} \tag{3.6b}$$

Most trajectories belonging to case (a) are stable, except for a set of measure zero corresponding to a few very simple values of α [13]. All trajectories belonging to case (b) are unstable. Consider case (a) with $\alpha = b/m$, where b and m are integers, and b/m is an irreducible fraction. Let $\mu_3(0)$ be the eigenvector for eigenvalue λ_3 of $M(\tau_0)$. Then $\mu_3(0)$ is also an eigenvector of $M(m\tau_0)$ for eigenvalue 1. In other words, we have found a neighboring orbit of $w_0(t)$, namely $w_0(t) + \mu_3(t)$ with $\mu_3(t)$ assumed small, which is periodic with period $m\tau_0$. This new periodic orbit "branches off" or "bifurcates from" the original periodic family which contains $w_0(t)$. This branching occurs at the point in the family where $\alpha = b/m$. If α is irrational, on the other hand, the orbit $w_0(t) + \mu_3(t)$ is not periodic, but it remains on a torus, provided $\mu_3(t)$ is small enough to keep chaos away, as suggested by the KAM theorem.

Figure 3.1 shows a generic Poincaré section in the neighborhood of a periodic orbit with α close to 1/6. The word "generic" in this context means that the problem is devoid of special symmetries. The dark points and the crosses represent the stable and unstable orbits, respectively, which have branched off the main orbit at $\alpha = 1/6$. Each of these points is a fixed point of $\mathcal{P}^6$ (if $\mathcal{P}$ is the Poincaré map). The continuous lines are invariant curves of $\mathcal{P}^6$: under successive iterations, points on these curves move along the curve in the direction of the arrow. The topology of the invariant curves becomes very complicated in the vicinity of the unstable fixed points, giving rise to a chaotic layer in this vicinity [1, 10]. According to Ref. [12], the width Δ of the "islands" for the generic case varies like

$$\Delta \propto \varepsilon^{m/4-1}, \tag{3.7}$$

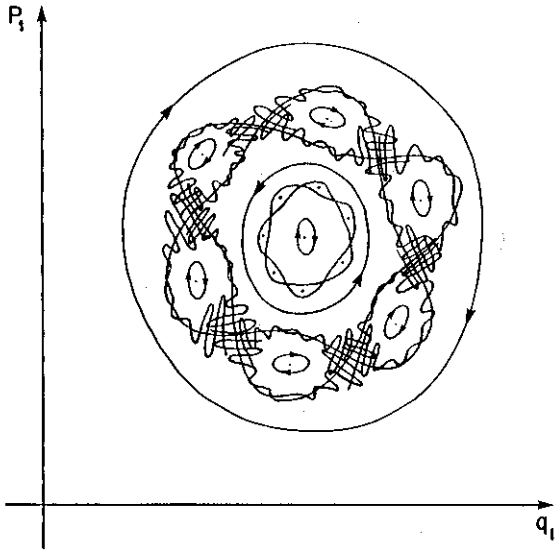

FIG. 3.1. Poincaré section just above a period sextupling bifurcation.

where ε, the "bifurcation parameter," is $\varepsilon = E - E_0$, E being the actual energy at which the Poincaré map is drawn, and E_0 being the bifurcation energy, such that $\alpha(E_0) = b/m$. Therefore, the bigger m is, the slower is the growth of the islands with energy, and the thinner are the chaotic layers surrounding the unstable points. If the width is small, the proportion of destroyed tori in the neighborhood is also small, and the bifurcated periodic orbits, both stable and unstable, are good approximations to the remaining tori.

According to Refs. [6, 14], the trace of the monodromy matrix of the bifurcated trajectory, in the vicinity of $\varepsilon = 0$ and provided $m > 4$, is given by

$$\operatorname{Tr} \mathcal{M}(\varepsilon) = 4 + A\varepsilon^{m/2}, \tag{3.8}$$

where A is a parameter depending on the particular branching. Combining this with Eq. (3.7), we see that $\operatorname{Tr} \mathcal{M}$ and the width Δ of the islands in the Poincaré section are connected by

$$\operatorname{Tr} \mathcal{M}(\varepsilon) - 4 \propto \Delta^{2/(1-4/m)}. \tag{3.9}$$

This gives us a quantitative criterion to decide when the bifurcated periodic orbit ceases to be a good approximation to the neighboring tori: we just look at the trace of its monodromy matrix! As long as $\operatorname{Tr} \mathcal{M}$ stays close to 4, the approximation is good; when it goes far from 4, the approximation is bad. The question "How far from 4 can we go?" will be seen to be not very important, because the transition between 4 and non-4 is quite sudden (see for instance Fig. 5.3). Notice that our

criterion is essentially the same as the "residue criterion" derived by Green [3] for two-dimensional conservative maps.

The validity of this criterion can be understood in another way, which was first formulated by James H. Mahoney. Figure 3.2 shows a high-m bifurcated periodic trajectory which approximates a torus very well. The trajectory of the original family follows the center line of the torus. Consider the $\mathcal{M}$ matrix of the bifurcated trajectory, which is defined by Eq. (3.5) with $t = \tau_0$. As always with periodic trajectories, one can choose the small displacement $\xi(0)$ in the direction of the trajectory itself; the perturbed trajectory is then identical to the original periodic one, and this fact is responsible for the two eigenvalues $\lambda_1 = \lambda_2 = 1$ of the $\mathcal{M}$ matrix. But, as Fig. 3.2 shows, there is another small displacement $\xi(0)$ which leads to the identical trajectory, namely a sideways displacement as far as the next winding of the trajectory on its torus. This displacement is not infinitesimal, therefore it leads to $\lambda_3 = \lambda_4 = 1$ approximately only. But if m is large, this displacement is very small and the approximation is very good, and then $\operatorname{Tr} \mathcal{M}$ is very close to 4.

As long as our trajectory remains a "quasi-torus," $\operatorname{Tr} \mathcal{M}$ remains close to 4. Eventually, and rather suddenly, as we vary the energy away from the bifurcation point, our quasi-torus decides to evolve into something else, which does not look like a torus anymore, but which is still a periodic trajectory. At this point we stop calling it a "quasi-torus" and we start calling it a "main periodic trajectory." The latter are of two kinds, of course, stable and unstable, and the Poincaré–Birkhoff theorem [1] says that we have equal numbers of each. If $\operatorname{Tr} \mathcal{M}$ drops below 4, the trajectory is stable and starts developing its own set of "second-order" nearby tori. This process continues indefinitely, accumulating very fast in the region of the fractal boundary between regular motion and chaos in phase space. Eventually (and usually rather quickly), $\operatorname{Tr} \mathcal{M}$ reaches 0, where a stable period-doubled trajectory branches off, while the first trajectory becomes unstable. On the other hand, if we leave the quasi-torus mode by having $\operatorname{Tr} \mathcal{M}$ increased beyond 4, the resulting main periodic orbit is an unstable one, which is surrounded in phase space by chaos.

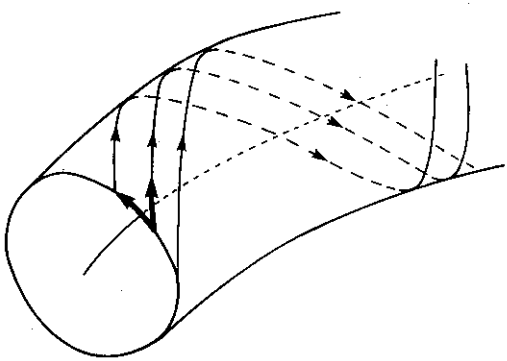

FIG. 3.2. Quasi-torus winding on a torus-like surface.

We want to emphasize that the numerical techniques we use to calculate quasi-tori are essentially the same that were used in Refs. [6, 8, 9] to calculate simple periodic trajectories. A complete description of the method can be found in Ref. [9]. The only important modification is that, now, not only can we follow a quasi-tori family by changing its energy and keeping its rotation number fixed, which is what the old programs do automatically, but we have developed new techniques to change the rotation number as well. In both cases, we use a previously calculated quasi-torus as a first approximation for the next one. To change the rotation number, we also change the number of points on the next quasi-torus, in order to keep approximately constant the average number of points per winding, or the time-step between two consecutive points.

When we change the rotation number, we are actually jumping from one periodic family to another. An obvious, but absolutely impractical, way to achieve this jump would be to decrease the energy of the original quasi-torus family until it branches upon the main family, then follow the main family until we get to the right value of α to fit the new rotation number, then branch off at this point to a quasi-torus family and raise the energy until it reaches its original value. (Note: α and the rotation number are essentially the same thing; their precise relationship is discussed in the next section.) In this process, we do not jump at all: we make continuous, but complicated, moves among the periodic families. However, if we did only this, we would never be able to find the tori connecting two distinct main families. To see how the jump can be achieved more directly, let us call $\rho_1 = b_1/m_1$ the rotation number of the original quasi-torus, and let us try to jump to $\rho_2 = b_2/m_2$. We assume, of course, that ρ_2 is close to ρ_1, which does not mean at all that m_2 is close to m_1, or that b_2 is close to b_1. (For example, we might wish to jump from 5/17 to 7/23.)

Figure 3.3 is a Poincaré section in the neighborhood of these quasi-tori. It shows two closed chains of thin islands, very close to each other, but with very different

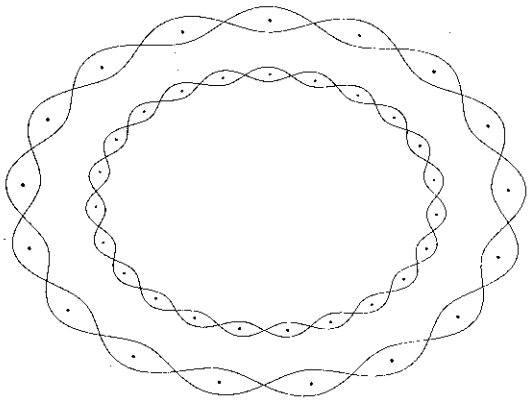

FIG. 3.3. Two nearby quasi-tori. The width of the islands has been intentionally enlarged for easier visualization.

numbers of islands, m_1 and m_2. The angles of rotation around each chain for successive crossings of the plane are, however very similar, since they are $2\pi\rho_1$ and $2\pi\rho_2$. Therefore, if we know quasi-torus 1, and we want to calculate quasi-torus 2, we can use quasi-torus 1 as a starting guess for the calculation, but we propagate the particle through m_2 crossings of the plane, rather than m_1. The resulting rotation angle is $2\pi\rho_1 m_2 = 2\pi(\rho_1/\rho_2)\, b_2$, which is almost a multiple of 2π since ρ_1/ρ_2 is close to unity. Hence this trajectory is almost closed, and the methods of Ref. [9] can turn it easily into a closed trajectory.

This is how we have done all our calculations. The method works very well as long as ρ_1 and ρ_2 are close. And it works even better if m_2 is a prime number. Otherwise, if m_2 has a divisor, say d_2, it may happen that, instead of getting a trajectory which crosses the plane m_2 times, we get one with m_2/d_2 crossings, described d_2 times. This is especially likely to happen if $b_2 - 1$ or $b_2 + 1$ is divisible by d_2.

Now that we know how to calculate quasi-tori, we have to learn to extract information from them. In the next section, we shall see how the actions can be calculated.

IV. The Basic Loops and the Actions

The actions are usually defined as integrals $\oint p \cdot dq$ along closed curves on the torus, and it is known [15] that topologically-equivalent closed curves yield the same action. But a torus has many topologically-inequivalent closed curves! Which two should be chosen? This problem is not trivial and, in order to think about it well, it is *not* a good idea to view the torus as a donut in three-dimensional space. Our torus is in four-dimensional phase space, and it is a very different species of animal. The donut in three-dimensions has two very special basic loops; our torus in four-dimension does not!

What results is that there is no unique pair of topologically-inequivalent closed curves along which we are to calculate $\oint p \cdot dq$. But neither can we choose any pair whatsoever. The fact is that there exists on the torus a special class of pairs of closed curves, which the topologists call "the possible bases for its fundamental group" [19]. This class is very important in physics, because we must choose a pair from this class when we want to define action-angle variables, and we must choose a pair from this class when we want to carry out EBK quantization [20]. The Appendix discusses in more detail how this class is defined. In what follows, we assume that the reader has read the Appendix.

From the previous discussion, we know that there is a family of tori associated with each family of stable periodic orbits. We can use this fact to pick one of the two basic loops on the tori, namely that loop which, in a very thin torus, is "perpendicular" to the main trajectory around which the torus winds. The requirement is simply that this loop must shrink to a point in the limit in which the torus shrinks to the main trajectory; in addition, the loop must not repeat itself. This

defines the loop uniquely, topologically speaking. Let us call it γ_s. Let us call γ_l another loop, which reduces in the limit to the main periodic trajectory. These form a possible pair of basic loops. But, according to Eqs. (A.4) with $n_1 = 1$, $n_2 = 0$, the combination

$$\gamma_b = \gamma_s \tag{4.1a}$$

$$\gamma_m = \gamma_l + k\gamma_s, \qquad k \text{ any integer}, \tag{4.1b}$$

is equally acceptable as a pair of basic loops. Thus the actions

$$J_b = \oint_{\gamma_b} p \cdot dq \tag{4.2a}$$

$$J_m = \oint_{\gamma_m} p \cdot dq, \tag{4.2b}$$

which we use to label the tori within their family, contain the arbitrary integer k (i.e., J_m is undetermined by the amount kJ_b).

In the special case (which includes integrable systems) in which the family of tori is bounded by *two* main periodic families, k gets determined by the requirement that J_m go to zero as the torus tends toward the other main orbit. Otherwise, we just have to pick k arbitrarily and keep it fixed from there on.

Now that a pair of basic loops has been chosen, we need to discuss the connection between the rotation number and the stability angle $2\pi\alpha$. Every quasi-torus, i.e., every periodic trajectory which can be recognized as an approximate torus, can be considered as topologically equivalent to n_1 times the loop γ_1 plus n_2 times the loop γ_2. Its rotation number can be chosen to be either n_1/n_2 or n_2/n_1, at will. Let us look at the way in which a family of quasi-tori branches off from a main periodic family. This was described in Section III, following Eqs. (3.6). The quantity α which appears in (3.6a) is undetermined by an integer, just like the number k in (4.1b). It does not have to be between 0 and 1. And, actually, the best choice for α is to take the rotation number of the quasi-torus, b/m: here m is the number of times that the trajectory winds around the "main" loop γ_m, first defined in (4.1b), which is the large loop of the torus, paralleling approximately the trajectory of the main family; and b is the number of times that the trajectory winds around the "branch" loop γ_b, first defined in (4.1a), which is the small loop created by the time-variation of $\mu_3(t)$. The indeterminacy in the definition of γ_m, manifested by the appearance of the arbitrary integer k in Eq. (4.1b), entails an indeterminancy in the integer b by an amount km. Hence b/m, like α, is defined up to an integer. Note that γ_b and γ_m have two very distinct roles, and the natural way to make a Poincaré section is in the plane of γ_b. As the quasi-torus grows in thickness away from the main trajectory, the importance of the distinction between γ_m and γ_b will decrease. If we change the rotation number by the method described previously, and if there is a connection with a different main family, the roles of the two loops will eventually get reversed,

γ_b will become $\gamma_{m'}$ for the new main family, while γ_m will become $\gamma_{b'}$. At this point, the integer k will get determined by the requirement that loop γ_b shrink to a point on the new main family.

This discussion can be summarized as follows. Near its branching from a main family, the rotation number of a quasi-torus is the same as α, the stability angle divided by 2π, and it is undetermined by an integer. Far from such branching, any one of the fractions α, as well as all their inverses, have equal claims to being called the rotation number. In the event that the other side of the family of quasi-tori branches again upon another main family, then one of the inverses becomes singled out as the only correct one.

We are now in a position to identify the two basic loops belonging to a numerically calculated quasi-torus. Let us start with a very thin quasi-torus, newly branched off from a main periodic family of period τ_0, number of points N_0, time-step $\varepsilon_0 = \tau_0/N_0$. With α chosen as mentioned above, the period of the quasi-torus is approximately $\tau = m\tau_0$, but we want its time-step to remain the same as that of the main orbit, $\varepsilon = \varepsilon_0$, therefore its number of points must be $N = mN_0$. Figure 4.1 illustrates the result of the numerical bifurcation, for one of the branchings from the main "horizontal" family of MARTA, with $m = 23$, $b = 37$, $N_0 = 48$. In Fig. 4.1a, the 23×48 points are linked by line segments, which has the effect of emphasizing the whole orbit. In Fig. 4.1b the same points are left unlinked, and we see then that the points group themselves into loops in planes perpendicular to the main orbit. Any one of these loops can be used as loop γ_b, which is thus very easy to obtain: its points are separated by intervals of N_0 steps along the quasi-torus trajectory, and it contains m points. The other basic loop γ_m is a little bit more complicated: we start at a point of loop γ_b and we include every point of the trajectory until we come back to γ_b for the first time, then we close the loop by walking b steps along γ_b, returning to the original point, as shown in Fig. 4.1c. This is an unsmooth version of γ_m: the first part of it, from γ_b and back to γ_b, contains N_0 steps; the second part, back to the original point along γ_b, should contain b steps; the total number of steps, or of points, is thus $N + b$. In order that this γ_m correspond exactly to the definition (4.1b), with the value of k that we chose there, or equivalently in order that the rotation number be the one we chose, it is important that the second part of γ_m have exactly b steps, rather than $m - b$, or $b - m$, or anything else: these are just the steps *backward* that are necessary to cancel out the γ_b rotation in the first part.

As we raise the energy away from the branch point on the main family, the quasi-torus gets continuously thicker, but the above definitions of the basic loops get extended by continuity. Similarly, as we change the rotation number by small jumps, the identity of the basic loops remains clear, and they are thus defined for the entire quasi-torus family. Figure 4.2 shows the process of constructing them for a quasi-torus issued from the vertical MARTA family.

Once we have found the basic loops, the calculation of the actions by Eqs. (4.2) is obvious. It is clear that the values of the actions will not be accurate unless m is a fairly large number. Using $m = 2$ or 3, for instance, would give very poor

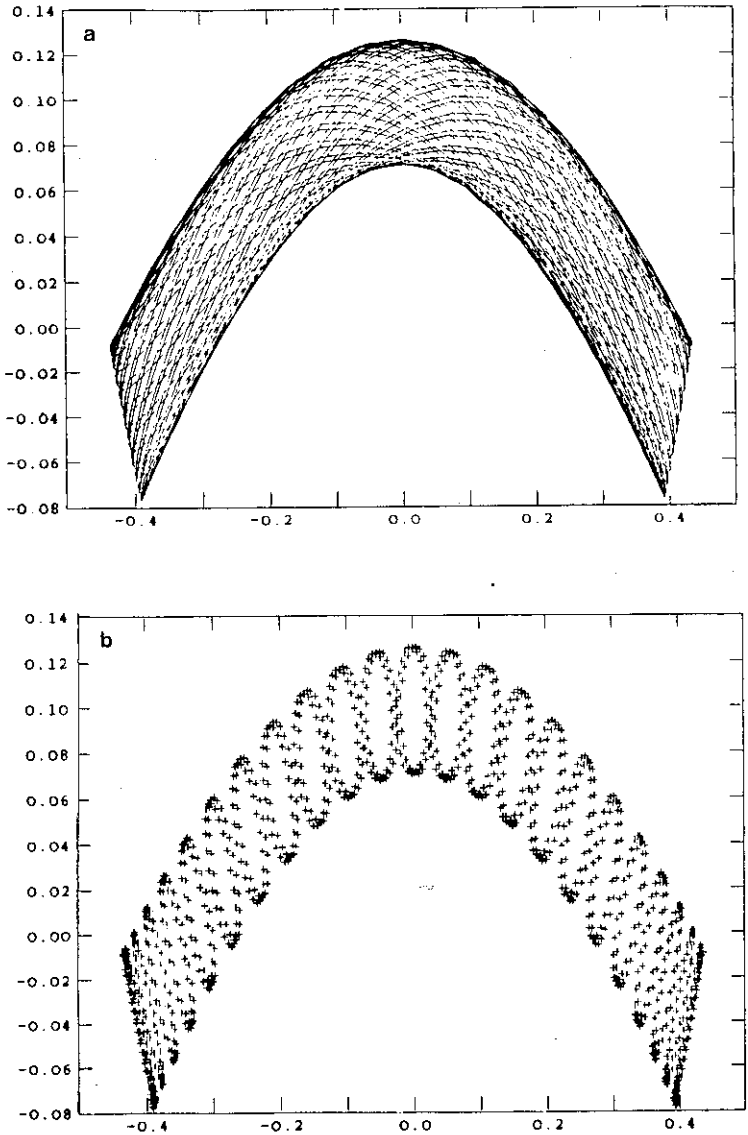

FIG. 4.1. Quasi-torus with $\rho = 23/37$. In part (a) the points are linked by line segments. Part (b) shows the same points unlinked and, in part (c), the loop γ_m is shown by a solid line. Note that, because $b > m$, the unwrapping along γ_b involves one complete loop (m points), plus $b - m$ additional points, for a total of b points.

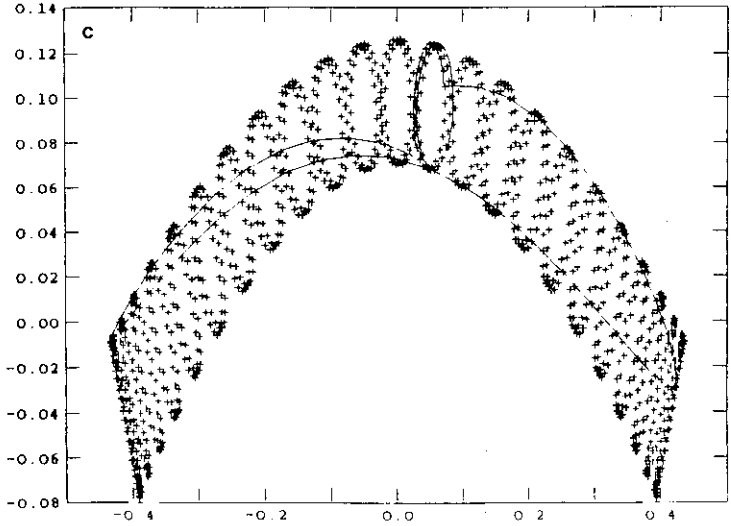

FIG. 4.1—*Continued.*

approximations to the actions of the nearby tori. In our calculations, we have used $N_0 = 48$ almost always, and m mostly around 25, but we also have some quasi-tori with m as large as 64, as Fig. 4.3 shows.

There is no physical significance to the fact that, in the above numerical construction of the basic loops, γ_b is smooth and γ_m is unsmooth. It is simply due to the choice of the total number of points on the trajectory, namely mN_0, which is a multiple of m. We can then construct γ_b by taking every N_0th point, and it is smooth. If we had chosen a multiple of b for the total number of points, say bP_0, then we could obtain a smooth γ_m by taking every P_0th point. This is precisely what happens for a quasi-torus belonging to a family of quasi-tori which connects two main periodic families. Then, the same quasi-torus can be reached from both sides. Consider, for instance, the two-dimensional family of tori which joins the horizontal (H) periodic family and the vertical (V) periodic family in MARTA or NELSON. Let a particular quasi-torus have rotation number $\rho = b/m$ when coming

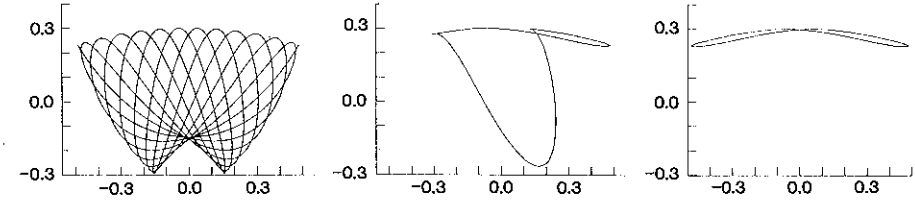

FIG. 4.2. The two loops for a vertical quasi-torus with $\rho = 15/26$. In this case $b < m$ (compare with Fig. 4.1 where $b > m$).

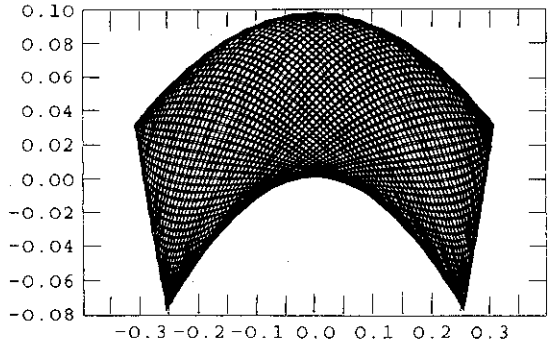

FIG. 4.3. A quasi-torus with $\rho = 64/107$.

from the H family, and rotation number $\rho' = b'/m'$ when coming from the V family, with $b' = m$, $m' = b$. (Recall that, now, there is no more indeterminancy in k, α, or b.) Suppose that we have used the same number of points, N_0, for both main families. Then, our two calculations of this quasi-torus have different total numbers of points (and therefore different points altogether). When coming from H, we have mN_0 points, the γ_b loop is smooth, but γ_m is unsmooth. When coming from V, we have $m'N_0$ points, which is bN_0, and the smooth loop is $\gamma_{b'} \equiv \gamma_m$, the unsmooth loop is $\gamma_{m'} \equiv \gamma_b$. The two actions, however, should be approximately independent of the calculation.

Of course, there is one obvious way to get both loops to be smooth in the same calculation, which is to use for total number of points a multiple of both m and b. This may force us to use different N_0's for different quasi-tori, which is a tricky and time-consuming thing to do, but it works. In Fig. 4.4, we show a quasi-torus with rotation number 26/45 and total number of points $N = 2340 = 26 \times 45 \times 2$. The two loops γ_m and γ_b can both be made smooth and have 45 and 26 points, respectively (last column of Fig. 4.4). This quasi-torus was actually calculated in two different

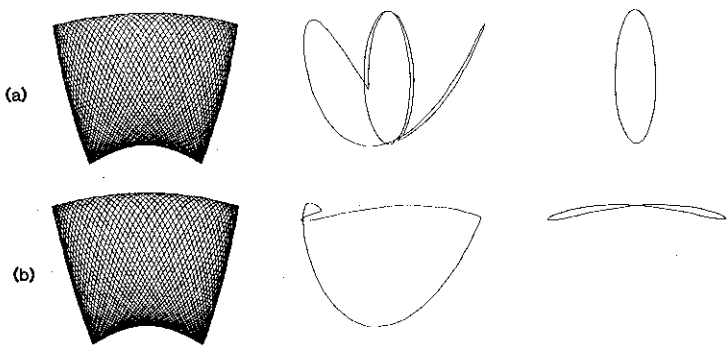

FIG. 4.4. The quasi-torus $H45/26$ with 2340 points. Because 2340 is a multiple of both 45 and 26, the two loops can be made smooth.

ways. For part (a), first row of Fig. 44, we started from the H main family with $N_0 = 90$, we looked for the branching at $\alpha = 45/26$ and we increased the energy at constant ρ until $E = E_0$. For part (b), second row of Fig. 4.4, we started from a quasi-torus close to the V family, with $N_0 = 52$, and changed the rotation number at this same energy, E_0 say, until $\rho = 26/45$. The total number of points, $2 \times 26 \times 45$, is the same in both cases, and they are the same points, except for an overall sliding along the trajectory due to finite numerical precision amounting to 0.6 % of a time-step. The construction given earlier yields one smooth and one unsmooth basic loop in each case, but obviously we can choose the two smooth loops. The actions should be the same with both calculations. If we call γ_H the loop which reduces to the H main family in the limit of a very thin torus, and γ_V the loop which reduces to the V family, we find

$$J_H(\text{smooth}) = 0.0895 \qquad J_H(\text{unsmooth}) = 0.0901$$
$$J_V(\text{smooth}) = 0.0851 \qquad J_V(\text{unsmooth}) = 0.0857.$$

The loop γ_V(unsmooth) has $52 + 45 = 97$ points, γ_H(unsmooth) has $90 + 26 = 116$ points, γ_H(smooth) has 26 points, and γ_V(smooth) has 45 points. The accuracy is not perfect but the error is less than 1 % for both J_H and J_V. It would improve even more if we used more points.

V. Numerical Results

We shall now present the results of numerical calculations of quasi-tori in the MARTA potential. The Hamiltonian is given in (1.1). At low energies it can be approximated by two independent harmonic oscillators of frequencies $\omega_x = 1$, $\omega_y = \sqrt{3}$. These frequencies are slightly modified when a discrete time-mesh is used; see Ref. [9, Sect. 7]. The harmonic oscillation in the y direction is actually exact at all energies and constitutes what we have called the vertical family of main periodic orbits. The x-oscillation, on the other hand, couples with the vertical degree of freedom as the amplitude increases, and the trajectory assumes the "boomerang" shape shown in Fig. 5.1, forming what we call the horizontal family.

The vertical and the horizontal orbits are the two main periodic families at low energy. Below $E = 0.8$ (the saddle points are at $E = 0.75$), all other periodic families can be obtained by bifurcation from one of these two. Both families are stable at low energy, and between them we find a family of tori that we call the "bottom family." At higher energies there are many other stable periodic families, each of them surrounded by a two-parameter family of tori, but most of our study was done with the bottom family.

We found that the bottom family of tori connects the V and H periodic families, and that most tori bifurcated from V continue to exist for energies higher than the energy at which V itself becomes unstable. Figure 5.2 shows $x - y$ projections of

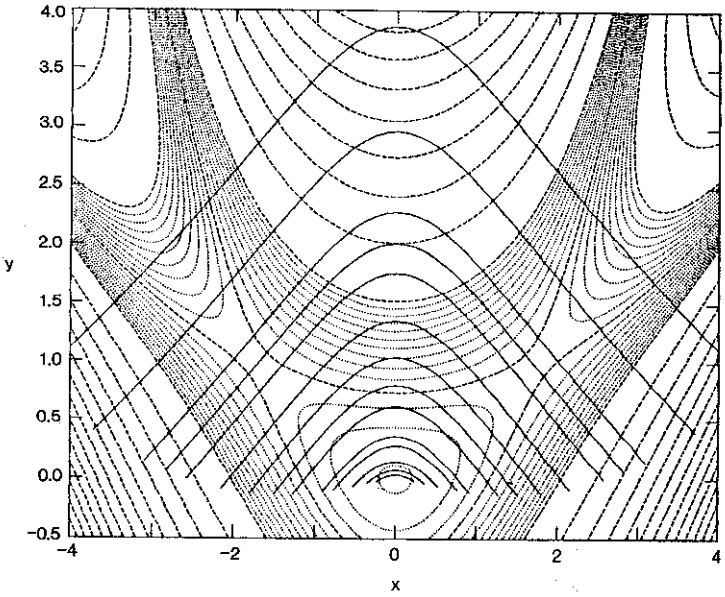

FIG. 5.1. $y-x$ plot of some trajectories of the H family superimposed over the equipotential lines of the MARTA potential.

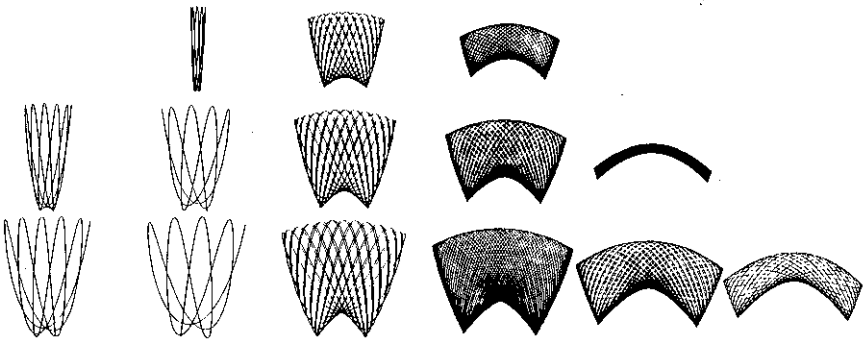

FIG. 5.2. $y-x$ projections of several tori in the bottom family. The rotation number changes horizontally and the energy vertically. The three rows, from top to bottom, have energies 0.05, 0.08, and 0.11, respectively. The columns, from left to right, are $V6/11$, $V5/9$, $V15/26$, $H52/31$, $H44/27$, and $H37/23$.

these quasi-tori, labeled with the notation Fb/m, where F stands for either V or H, and b/m is the rotation number in the notation of Section IV. Three different energies are shown, with a variety of rotation numbers for each energy. In this figure we have intentionally plotted two quasi-tori with rather simple rotation numbers, namely, $V6/11$ and $V5/9$ (see caption). These quasi-tori clearly show one important difference between a real torus and a highly winding orbit: its symmetry. As shown in Refs. [6, 16], orbits bifurcated from symmetric librations with period n-upling, may lose one of their symmetries, depending on whether n is even or odd. The real tori of the bottom family, on the other hand, always have the $x \to -x$ and time reversal symmetries. So, a symmetric torus may eventually be approximated by an asymmetric orbit. For the bottom family, it turns out [6, 16] that there are three different kinds of n-upled orbits: symmetric librations, asymmetric librations, and symmetric rotations. Of course, if the number of windings is big enough, these three kinds of orbits become undistinguishable in practice, as is the case with the other quasi-tori in Fig. 5.2.

As we increase the energy above $E=0.1$, which is approximately where V becomes unstable, the bottom family of tori cannot touch the V main family anymore, but the tori approximated by Vb/m are still connected with the H main family. If we try to push them toward V at constant energy, these tori break down into chaos in a way which is described with some detail in Ref. [17]. Their quasi-tori approximants, however, will continue to exist in the form of main families of periodic orbits. It is important to note that our method allows us to calculate quasi-tori labeled by Vb/m even when V itself is already unstable.

Figure 5.3 is a plot of Tr $\mathcal{M}$ versus energy for the quasi-torus $H45/26$. Note that the point where Tr $\mathcal{M}$ becomes different from 4 is quite well-defined: the transition is very sudden. From that point on, the orbit stops being a good representation of a

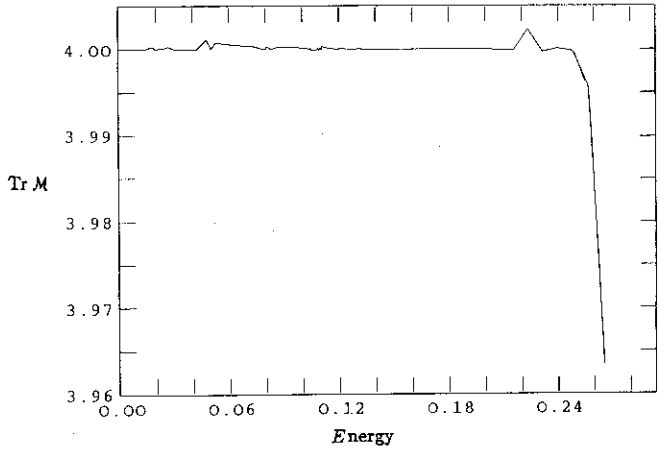

FIG. 5.3. Tr($\mathcal{M}$) × Energy for $H45/26$ showing the sudden transition between the "4" and "non-4" regions. The oscillations are due to numerical imprecision.

torus and starts to develop its own family of second-order tori. The same transition occurs for all our orbits, but the energy where it occurs is highly dependent on the rotation number, as discussed in Sections II and III.

The connection between V and H through the bottom family is displayed with action coordinates on Fig. 5.4. The energy contours are the very slightly convex lines which span the diagram with a negative slope. Recall that the slope of the normal to such a contour is the rotation number, according to Eq. (2.1). Note that, if we lower the energy of the torus at constant rotation number, we end up with a branching upon either the V family, represented by the horizontal axis, or the H family, represented by the vertical axis, but not both. In other words, the tori of the bottom family can be classified into two categories according to rotation number: those with $\rho < 1/\sqrt{3}$ arise by branching from the V family and raising the energy; those with $\rho > 1/\sqrt{3}$ arise by branching from the H family and raising the energy. (Here we have defined ρ such that $\rho < 1$, which corresponds to $\rho = b/m$ in the vicinity of V, but to $\rho = m/b$ in the vicinity of H.) We see, therefore, that in the notation Fb/m which we use for a quasi-torus of the bottom family, F is unique, either V or H. Moreover, if $(1/\sqrt{3})_r$ is a rational approximation to $1/\sqrt{3}$, $V(1/\sqrt{3})_r$ is contiguous to $H(\sqrt{3})_r$.

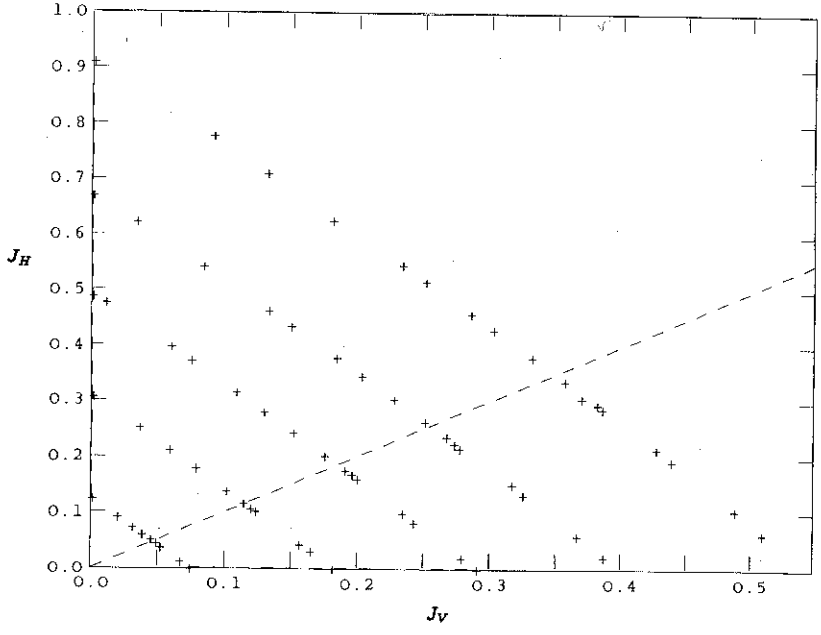

FIG. 5.4. $J_H \times J_V$ plot of MARTA's bottom family. The lines $J_V = 0$ and $J_H = 0$ correspond to the horizontal and vertical periodic orbits, respectively. The energy contours are at $E = 0.03$, $E = 0.05$, $E = 0.08$, $E = 0.11$, and $E = 0.15$. Note that the last two contours are not touching the vertical family, which becomes unstable at $E \simeq 0.10$.

As we said earlier, for each periodic trajectory labeled by Fb/m there exists an energy at which it stops "behaving like" a torus to become an ordinary periodic orbit. This means that a whole neighborhood of the destroyed rational torus Fb/m is also being destroyed by the non-linearity of the equations of motion. If we were to mark this transition point for every periodic orbit in the (J_H, J_V) plane, we would get a very complicated line separating the bottom family of tori from a region containing lots of unstable orbits surrounded by chaotic regions. Note that this line is *not* the boundary between the regular and chaotic regions, because roughly half the remaining periodic orbits are still stable, at least for a while, with second order tori around them, etc. .... But this line is the boundary between what we might call "the mostly regular region" and the rest of phase space. It is "mostly regular" because every periodic orbit in this region is either a main periodic orbit with $0 < \mathrm{Tr}\, \mathscr{M} < 4$, or a quasi-torus with all four eigenvalues of $\mathscr{M}$ close to unity.

Unfortunately, this boundary cannot be drawn in the plane of the actions, the reason being that, as we saw in the last section, we cannot make a good calculation of the actions of Fb/m when m is a small number. Orbits with small m, however, should be very important to the curve we are trying to draw, since they are the main sources of chaos. Therefore, we shall introduce new variables, τ_b and τ_m, whose accuracy does not depend on m being large. These are the partial periods simply defined by

$$\tau_b = \tau/b, \qquad \tau_m = \tau/m,$$

where τ is the true period. The average time take by the particle to complete the loop γ_b once is τ_b, and similarly for γ_m and τ_m. Note that τ_b and τ_m should be continuous as one moves from irrational to rational rotation number and vice-versa, i.e., they do not distinguish between quasi-tori and real tori.

We shall transport our (J_H, J_V) curves at constant energy to a (τ_H, τ_V) plot. We call τ_H that partial period which, in the limit of a very thin torus around the H family, reduces to the period of the H family; similarly for τ_V. We shall call τ_H^F and τ_V^F the two partial periods of very thin tori surrounding the main family F ($\equiv H$ or V). In the continuum limit, we have (see Ref. [9] for modifications due to the finite time-mesh)

$$\tau_H^V(E) = (2\pi/\sqrt{3})/\alpha^V(E) \qquad \tau_V^V(E) = 2\pi/\sqrt{3}$$
$$\tau_H^H(E) = \tau^H(E) \qquad \tau_V^H(E) = \tau^H(E)/\alpha^H(E),$$

where $(2\pi/\sqrt{3})$ and $\tau^H(E)$ are the periods of the V and H main families, respectively, and $2\pi\alpha^V(E)$ and $2\pi\alpha^H(E)$ are their stability angles.

Figure 5.5 shows the (τ_H, τ_V) plot for the bottom family of quasi-tori. In this plot, the curves of constant energy are concave, and those of constant rotation number are straight lines. The end point of each of these straight lines corresponds to the energy where Tr $\mathscr{M}$ starts to become "non-4." If we connect these points by straight segments, we get an approximation to be boundary between the mostly

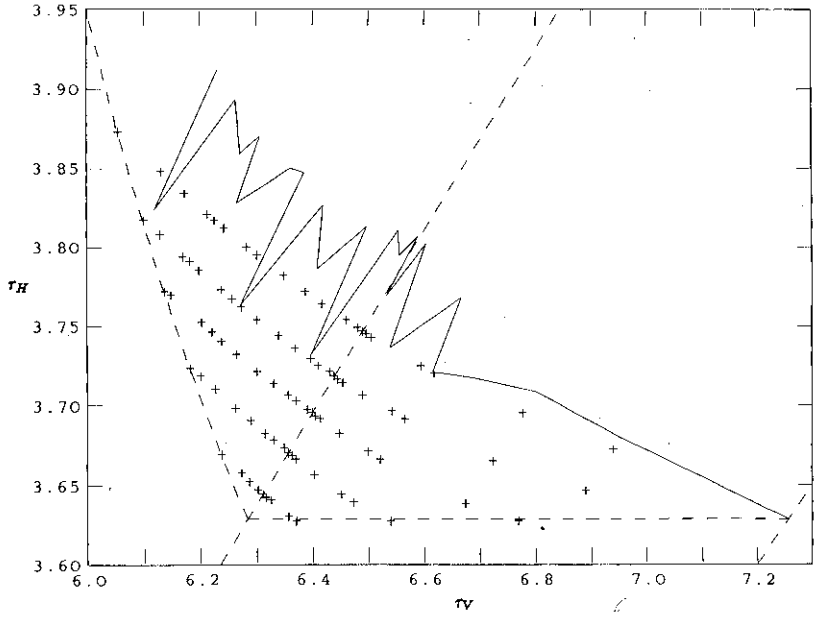

FIG. 5.5. $\tau_H \times \tau_V$ plot of MARTA's bottom family. The energy contours are the same as those in Fig. 5.4. The three big notches in the boundary curve correspond (from left to right) to *H*8/5, *H*5/3, and *H*12/7.

regular region and the rest of phase space. This is the zig-zagged curve of Fig. 5.5. The more points we take into account, the more zig-zags the curve will acquire, resembling a fractal in the limit. As expected, the deeper holes in the curve correspond to the simpler orbits, while the peaks represent more "complicated" rotation numbers (see the figure caption for more details).

The question of what happens to the periodic orbits after this boundary is reached turns out to be very interesting and non-trivial. Preliminary results show that, as the energy is increased beyond the boundary, some of the highly winding orbits start to wind around simpler nearby periodic orbits, as though phase-space had been "scarred" by the simpler orbit. This phenomenon of "classical scars" seems to be analogous to the "quantal scars" discovered by Heller [18], which consist of an accumulation of probability, for certain quantal stationary states, in the vicinity of some simple, periodic, classical orbit. These classical scars and their relationship with Heller's results are now being actively investigated.

VI. CONCLUSION

We have presented a method for calculating tori using periodic orbits. Its main advantage is that it allows the systematic calculation of any family of tori, not only

those existing in the integrable limit. Moreover, we can very easily calculate the two topologically independent circuits on the torus, and therefore the actions, without the necessity of using Poincaré sections.

Our results with the MARTA Hamiltonian show that the horizontal and vertical families of periodic trajectories are connected through tori. However, it is not very likely that all families of tori are bounded by two periodic orbits, as is the case for the MARTA bottom family. Some of them may be destroyed too fast, before reaching any other stable periodic family. A possible example of such behavior are the tori around the tiny stable branches of the vertical family (in MARTA or NELSON—see Refs. [6, 8]) occurring in high energies, where the phase space is mostly chaotic. On the other hand, we believe that there may be connections through tori between other families of periodic orbits, other than the horizontal and vertical families. A better place to look for such connections is the NELSON Hamiltonian where at least four different families of stable periodic orbits can be found at fairly low energies.

We also applied our method to the calculation of a non-obvious family of tori (a family that does not exist in the integrable limit) in the NELSON Hamiltonian, namely, the tori around the "I" family [8]. Although any energy surface containing a stable member of I possesses other unstable orbits, as well as chaotic regions, we had no numerical problems doing this calculation: everything works as well as in the regular region.

Finally, we repeat that the numerical methods used here to calculate quasi-tori are essentially those described in Ref. [9]. The major difference is that we had to develop a method to enable us to jump from one quasi-torus to another of different rotation number. This procedure, described at the end of Section III, allowed us to explore the two dimensions of a family of tori.

APPENDIX:
Topological Properties of Closed Curves on a Torus

The notations γ, γ', ... will denote individual closed curves on a torus T^2. The notations $\Gamma_1, \Gamma_2, \ldots$ will denote complete sets of topologically equivalent closed curves. We call $\gamma_1, \gamma_1', \ldots$ the individual members of the set Γ_1; we call $\gamma_2, \gamma_2', \ldots$ the members of Γ_2, etc. ... Therefore, if $\Gamma_1 \neq \Gamma_2$, γ_1 and γ_1' can be continuously deformed into one another, but neither can be continuously deformed into γ_2.

Now we wish to consider pairs of closed curves. Since we are only interested in topological properties, we shall represent an inequivalent pair by (Γ_i, Γ_j), with $i \neq j$, and with the understanding that any element γ_i of the set Γ_i can be used as the first member of the pair, and any element γ_j of Γ_j can be used as the second member.

Among all these pairs, there are some that have the following property: an arbitrary closed curve γ_p on the torus can be written as

$$\Gamma_p \doteq m_p \Gamma_i + n_p \Gamma_j, \tag{A.1}$$

where m_p and n_p are *integers* and $\doteq$ means "topologically equivalent." We shall call the pairs satisfying (A.1) "coordinate pairs." They are not unique; but neither do they include all possible pairs. We illustrate by an example.

Let the torus consist of all points

$$(x \text{ modulo } 1,\ y \text{ modulo } 1)$$

in the xy plane, and consider the following four closed curves

$$\begin{aligned}
\gamma_1(t_1) &= \{(x(t_1), y(t_1)) = (t_1, 0)\} \\
\gamma_2(t_2) &= \{(x(t_2), y(t_2)) = (0, t_2)\} \\
\gamma_3(t_3) &= \{(x(t_3), y(t_3)) = (t_3, t_3)\} \\
\gamma_4(t_4) &= \{(x(t_4), y(t_4)) = (t_4, -t_4)\}
\end{aligned} \tag{A.2}$$

with $0 \leqslant t_i < 1$. Fig. A.1 displays the four curves. It is easy to see that the pairs (Γ_1, Γ_2), (Γ_1, Γ_3), (Γ_1, Γ_4), (Γ_2, Γ_3), (Γ_2, Γ_4) all satisfy (A.1), but (Γ_3, Γ_4) does not. To show the latter, it is enough to note the relation

$$\Gamma_1 \doteq \tfrac{1}{2}\Gamma_3 + \tfrac{1}{2}\Gamma_4 \tag{A.3}$$

which has non-integer coefficients.

In general, if (Γ_1, Γ_2) is a coordinate pair, all other coordinate pairs (Λ_1, Λ_2) can be generated by the equations

$$\Lambda_1 \doteq n_1\Gamma_1 + n_2\Gamma_2 \tag{A.4a}$$

$$\Lambda_2 \doteq n_3\Gamma_1 + n_4\Gamma_2, \tag{A.4b}$$

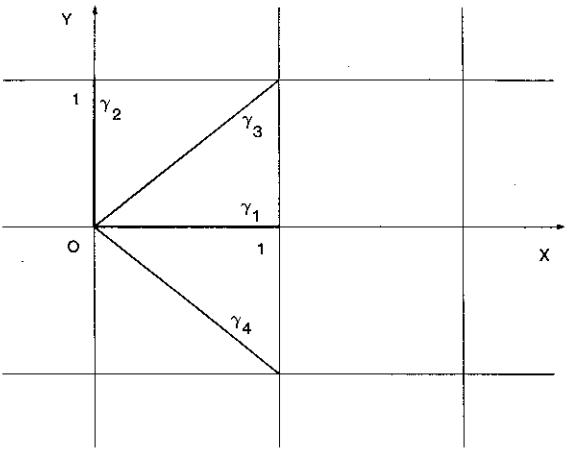

FIG. A.1. Four closed curves in the "unit square" torus.

where the n_i's are integers satisfying the relation

$$n_1 n_4 - n_2 n_3 = \pm 1. \tag{A.5}$$

That this is a sufficient condition is obvious, since it makes it possible to solve for (Γ_1, Γ_2) in terms of (A_1, A_2) with integer coefficients. To see that the condition is also necessary, let $n_1 n_4 - n_2 n_3 \equiv d$ be an integer different from ± 1. Since it must be possible to express (Γ_1, Γ_2) in terms of (A_1, A_2) with integer coefficients, we conclude that n_1, n_2, n_3, n_4 must all be multiples of d. Then, the following closed curve must exist on the torus,

$$\Sigma \doteq (n_1/d)\,\Gamma_1 + (n_2/d)\,\Gamma_3, \tag{A.6}$$

and Eq. (A.4a) gives us the relation

$$\Sigma \doteq \frac{1}{d} A_1. \tag{A.7}$$

But this contradicts the assumption that (A_1, A_2) is a coordinate pair, since the coefficient is not an integer.

Whenever we are looking for two curves on the torus to serve as "coordinate axes," we need to choose two members of a "coordinate pair," otherwise, the coordinates will not be one-to-one. For instance, referring to the curves of Fig. A.1, a point on γ_1 plus a point on γ_2 define a unique point on the torus, and vice versa. But this is not true of the pair (γ_3, γ_4): the points $t_3 = t_4 = 0$ and $t_3 = t_4 = 1/2$, for example, correspond to the same point on the torus. In mathematical terms, a coordinate pair on T^2 is a pair of generators for the "fundamental group" of the torus [19]. The fundamental group (or Poincaré group) has for elements all closed curves passing through a fixed point of a torus, and the group multiplication operation is the "+" used in the equations of this Appendix.

The "angle variables" of two-dimensional integrable Hamiltonian systems are an example of coordinate pairs in the above sense. The reader is referred to Arnold's book [15] for an extended treatment of the connection between angle variables and the fundamental group. Moreover, it can be shown that all EBK-like quantization rules need to be based on coordinate pairs of closed curves. For instance, in the case of two decoupled harmonic oscillators, quantization along the closed loops (γ_3, γ_4) of Fig. A.1 would yield extraneous and incorrect levels.

ACKNOWLEDGMENT

We would like to thank Jim Mahoney for helpful discussions and for giving us many hints on the use of the VAX computer and SPEAKEASY language.

REFERENCES

1. H. POINCARÉ, *Rend. Circ. Mat. Palermo* **33** (1912), 375; G. D. BIRKHOFF, *Trans. Amer. Math. Soc.* **14** (1913), 14.
2. V. A. YAKUBOVICH AND V. M. STARZHINSKII, "Linear Differential Equations with Periodic Coefficients," Keter Publishing House, Jerusalem, 1975.
3. J. M. GREENE, *J. Math. Phys.* **20** (1979), 1183.
4. D. W. NOID AND R. A. MARCUS, *J. Chem. Phys.* **62** (1975), 2119 and *J. Chem. Phys.* **67** (1977), 559; K. S. SORBIE AND N. C. HANDY, *Mol. Phys.* **32** (1976), 1327.
5. R. L. WARNOCK AND R. D. RUTH, *Physica D* **26** (1987), 1; S. CHAPMAN, B. C. GARRET, AND W. H. MILLER, *J. Chem. Phys.* **64** (1976), 502.
6. M. A. M. DE AGUIAR, C. P. MALTA, M. BARANGER, AND K. T. R. DAVIES, *Ann. Phys. (N.Y.)* **180** (1987), 167.
7. J. H. MAHONEY, Ph.D. thesis, MIT, Cambridge, MA, 1987, to be published; P. LEBOEUF, M. SARACENO, M. BARANGER, J. MAHONEY, AND D. PROVOST, submitted to *Phys. Rev. Lett.*
8. M. BARANGER AND K. T. R. DAVIES, *Ann Phys. (N.Y.)* **177** (1987), 330.
9. M. BARANGER, K. T. R. DAVIES, AND J. H. MAHONEY, *Ann. Phys. (N.Y.)* **186** (1988), 95.
10. V. I. ARNOLD AND A. AVEZ, "Ergodic Problems of Classical Mechanics," Appendix 34, Benjamin, New York, 1968; V. I. ARNOLD, "Mathematical Methods of Classical Mechanics," Appendix 8, Springer-Verlag, New York, 1978); M. V. BERRY, *in* "Topics in Non-Linear Dynamics" (S. Jorna, Ed.), American Institute of Physics, New York, 1978.
11. A. Y. KHINCHIN, "Continued Fractions" Univ. of Chicago Press, Chicago, 1964.
12. V. I. ARNOLD, "Mathematical Methods of Classical Mechanics," Appendix 7, Springer-Verlag, New York, 1978.
13. K. R. MEYER, *Trans. Amer. Math. Soc.* **154** (1971), 273.
14. K. R. MEYER, *Trans. Amer. Math. Soc.* **149** (1970), 95.
15. V. I. ARNOLD, "Mathematical Methods of Classical Mechanics," Chap. 10, Springer-Verlag, New York.
16. M. A. M. DE AGUIAR AND C. P. MALTA, *Physica D* **30** (1988), 413.
17. D. BENSIMON AND L. P. KADANOFF, *in* "Chaotic Phenomena in Astrophysics" (J. R. Buchler and H. Eichhorn, Eds.), p. 110, 1987.
18. E. J. HELLER, *Phys. Rev. Lett.* **53** (1984), 1515.
19. W. S. MASSEY, "Algebraic Topology: An Introduction," Chap. 2 and p. 89, Springer-Verlag, New York, 1987.
20. I. C. PERCIVAL, *Adv. Chem. Phys.* **36** (1977), 1.